Fractional Spin Excitations in the Infinite-Layer Cuprate $CaCuO_2$

Leonardo Martinelli,[1,*] Davide Betto,[2] Kurt Kummer,[2] Riccardo Arpaia,[3] Lucio Braicovich,[1,2] Daniele Di Castro,[4,5] Nicholas B. Brookes,[2] Marco Moretti Sala,[1] and Giacomo Ghiringhelli[1,6,†]

[1]*Dipartimento di Fisica, Politecnico di Milano, piazza Leonardo da Vinci 32, I-20133 Milano, Italy*
[2]*ESRF, The European Synchrotron, 71 Avenue des Martyrs, CS 40220, F-38043 Grenoble, France*
[3]*Quantum Device Physics Laboratory, Department of Microtechnology and Nanoscience, Chalmers University of Technology, SE-41296 Göteborg, Sweden*
[4]*Dipartimento di Ingegneria Civile e Ingegneria Informatica, Università di Roma Tor Vergata, Via del Politecnico 1, I-00133 Roma, Italy*
[5]*CNR-SPIN, Università di Roma Tor Vergata, Via del Politecnico 1, I-00133 Roma, Italy*
[6]*CNR-SPIN, Dipartimento di Fisica, Politecnico di Milano, I-20133 Milano, Italy*

(Received 12 October 2021; accepted 30 March 2022; published 19 May 2022)

We use resonant inelastic x-ray scattering (RIXS) to investigate the magnetic dynamics of the infinite-layer cuprate $CaCuO_2$. We find that close to the $(1/2, 0)$ point, the single magnon decays into a broad continuum of excitations accounting for about 80% of the total magnetic spectral weight. Polarization-resolved RIXS spectra reveal the overwhelming dominance of the spin-flip ($\Delta S = 1$) character of this continuum with respect to the $\Delta S = 0$ multimagnon contributions. Moreover, its incident-energy dependence is identical to that of the magnon, supporting a common physical origin. We propose that the continuum originates from the decay of the magnon into spinon pairs, and we relate it to the exceptionally high ring exchange $J_c \sim J_1$ of $CaCuO_2$. In the infinite-layer cuprates, long-range and multisite hopping integrals are very important, and they amplify the 2D quantum magnetism effects in spite of the 3D antiferromagnetic Néel order.

DOI: 10.1103/PhysRevX.12.021041 Subject Areas: Condensed Matter Physics

I. INTRODUCTION

The spin $1/2$ antiferromagnetic (AF) square lattice is one of the most studied systems in condensed matter theory, both for its exquisite quantum mechanical nature and for its implications in the longstanding problem of high T_c superconductivity in cuprates [1]. Despite the apparent instability in 2D, the magnetic ground state of these systems has been experimentally determined to be of Néel type, mostly thanks to weak interlayer exchange and Dzyaloshinskii-Moriya interactions [2–4]. Interestingly, the linear spin-wave theory (LSWT), which describes the magnetic excitations as spin-1 quasiparticles, provides an excellent description of the spin response in most of the 2D Brillouin zone [2,5–7] and of other static thermodynamic properties [8,9]. However, the region close to the magnetic zone boundary (related to short-wavelength physics) is known for deviating from this simple picture [2,10–12] with a sudden loss of magnon spectral weight and the build-up of a continuum at higher energies in the vicinity of the $(1/2, 0)$ point. These observations remain unexplained in LSWT, even when pushed to higher orders of $1/S$ expansion [13]. One possible interpretation is in terms of multimagnon processes, i.e., excitations involving a number of magnons greater than 1 [14–16]. Going beyond LSWT, multimagnons have indeed been successfully used to partially reproduce the experimental results, e.g., for $Sr_2CuO_2Cl_2$ [17].

However, several theoretical works have suggested that the peculiarities at the magnetic zone boundary arise from the proximity to some exotic nonmagnetic phases, such as the resonating valence bond (RVB) [11,18], the AF* [19], or valence bond solid (VBS) [20–22] states. The building blocks of these pure quantum mechanical ground states are pairs of spins arranged into local singlets [18], and their most fascinating property is the fractionalization of magnons into unbound (or almost-unbound) magnetic excitations carrying spin $1/2$, usually referred to as spinons. This spinon band is gapped in the Néel ground state, with a dispersion minimum at $(1/2, 0)$ where the magnon energy is maximum [11,19,22,23]. The mixing of the two bands at this wave vector might then transfer spectral weight from the magnon to the higher-energy spinon, giving rise to the continuum measured around $(1/2, 0)$ [22]. Indeed, at short wavelengths, minimally

*leonardo.martinelli@polimi.it
†giacomo.ghiringhelli@polimi.it

deconfined spinon pairs become more similar to magnons, and the two sorts of spin-1 excitations mix, similarly to an exciton-polariton scenario [22]. Whereas in 1D the separation (deconfinement) of two spinons has been observed in the case of spin-$1/2$ chains and ladders, in 2D, deconfinement is predicted to be only partial [22], unless the system is a spin liquid [21]. It has been proposed that such fractionalization might be present in the pure-Heisenberg AF compound copper deuteroformate tetradeurate, where the magnon anomaly has been clearly observed [11,22]. However, the experimental results were later accounted for using LSWT with a strong magnon-magnon interaction [16], casting doubts on the actual observation of spin fractionalization in that case. Therefore, to our knowledge, the existence of partially deconfined spinons in 2D square lattices has found no definitive experimental support so far. Cuprates are obvious candidates for the observation of fractional magnetic excitations: Although the RVB ground state originally proposed by Anderson [18] is challenged by the evidence of Néel AF order coming from neutron scattering and magnon dispersion, the $(1/2, 0)$ anomaly is a common feature. The magnetic Hamiltonian of cuprates arises from fundamental Hubbard-like physics [24–27] and entails couplings (schematized in Fig. 1) among first (J_1), second (J_2), and third (J_3) nearest neighbors, plus another multispin term that couples four spins across a Cu_4O_8 plaquette, usually called ring exchange [6,7,28]. It has been put forward that the partial deconfinement of spinons occurs in the presence of frustrating next-nearest neighbor [29–32] or multispin couplings [20–22,33]. In particular, many studies have established that J_c is by far the most important term [6,7,15]. Among cuprates, the infinite-layer $CaCuO_2$ (CCO) is characterized by the strongest long-range magnetic interactions, with a particularly large ring exchange J_c [7,34], so it is the ideal candidate in the quest for magnon fractionalization.

Although previous studies of CCO have already shown the presence of the anomaly and given an estimate of the J-values, highlighting the importance of the absence of apical oxygen in the structure [7], the actual nature of the anomalous spin spectrum still needs to be determined. Here, we study $CaCuO_2$ by resonant inelastic x-ray scattering (RIXS) at the Cu L_3 edge, exploiting several innovative techniques to unravel the properties of spin excitations at the $(1/2, 0)$ point; we find evidence that this anomaly is more consistent with a spinon pair continuum than with a multimagnon picture. Section II presents the technical experimental details of the measurements we perform, including information about samples growth, while in Sec. III, we present the results of our measurements. In particular, Sec. III A reports the momentum dependence of the energy and intensity of the magnetic excitations, which highlight a clear anomaly close to the $(1/2, 0)$ point. In Sec. III B, we present the results of our polarimetric measurements, which favor an interpretation of the anomaly in terms of fractionalization over multiple magnons. Finally, in Sec. III C, we report the incident-energy dependence of the magnetic spectrum, which further corroborates our interpretation. Section IV is devoted to the discussion and interpretation of the experimental results.

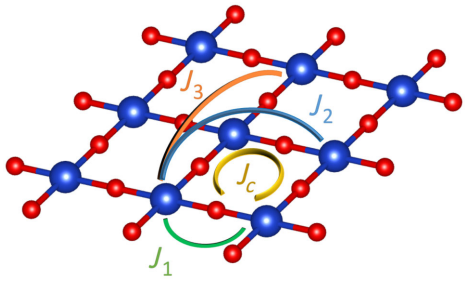

FIG. 1. Scheme of CuO_2 planes, with oxygen atoms depicted in red and copper atoms in blue. Colored lines highlight the magnetic coupling of the Hubbard-like Hamiltonian as explained in the text.

II. EXPERIMENTAL DETAILS

The crystal structure of $CaCuO_2$ displayed in Fig. 1 is the archetype of infinite-layer cuprates, with a stack of CuO_2 planes separated by Ca^{2+} cations. Cu^{2+} ions in the planes are in a $3d^9$ configuration, with spin $1/2$ and a single hole in the $3d$ shell. The absence of apical oxygen makes it almost impossible to dope this compound while preserving its special structure: Doping by extra oxygen leads to a complex unit cell [35]. Superconductivity has been obtained in heterostructures [36] and superlattices [37,38] by doping through the interface.

The CCO films were grown by pulsed-laser deposition (KrF excimer laser, $\lambda = 248$ nm) at a temperature around 600 °C and an oxygen pressure of 0.1 mbar, on $NdGaO_3$ (NGO) (1 1 0) substrate. The substrate holder was at a distance of 2.5 cm from the CCO target, which was prepared by a standard solid-state reaction [36,37].

The RIXS measurements were performed at the beam line ID32 of the European Synchrotron (European Synchrotron Radiation Facility, ESRF) in Grenoble (France), using the ERIXS spectrometer [39,40]. A schematic layout of the experimental geometry is depicted in Fig. 2(d). The CuO_2 plaquettes were kept perpendicular to the scattering plane, and we denote σ (π) the polarization perpendicular to (lying in) the scattering plane, with the addition of a prime symbol (σ', π') when referring to polarization of scattered photons. To carefully investigate the magnetic spectrum, we explored along all the degrees of freedom allowed by the RIXS technique: momentum transfer, incident-photon, and scattered-photon linear polarization directions [40], and incident photon energy close to the absorption peak. The results are presented and discussed in Secs. III A–III C, respectively.

The momentum dependence was mainly performed by rotating the angle θ while keeping the scattering angle (2θ)

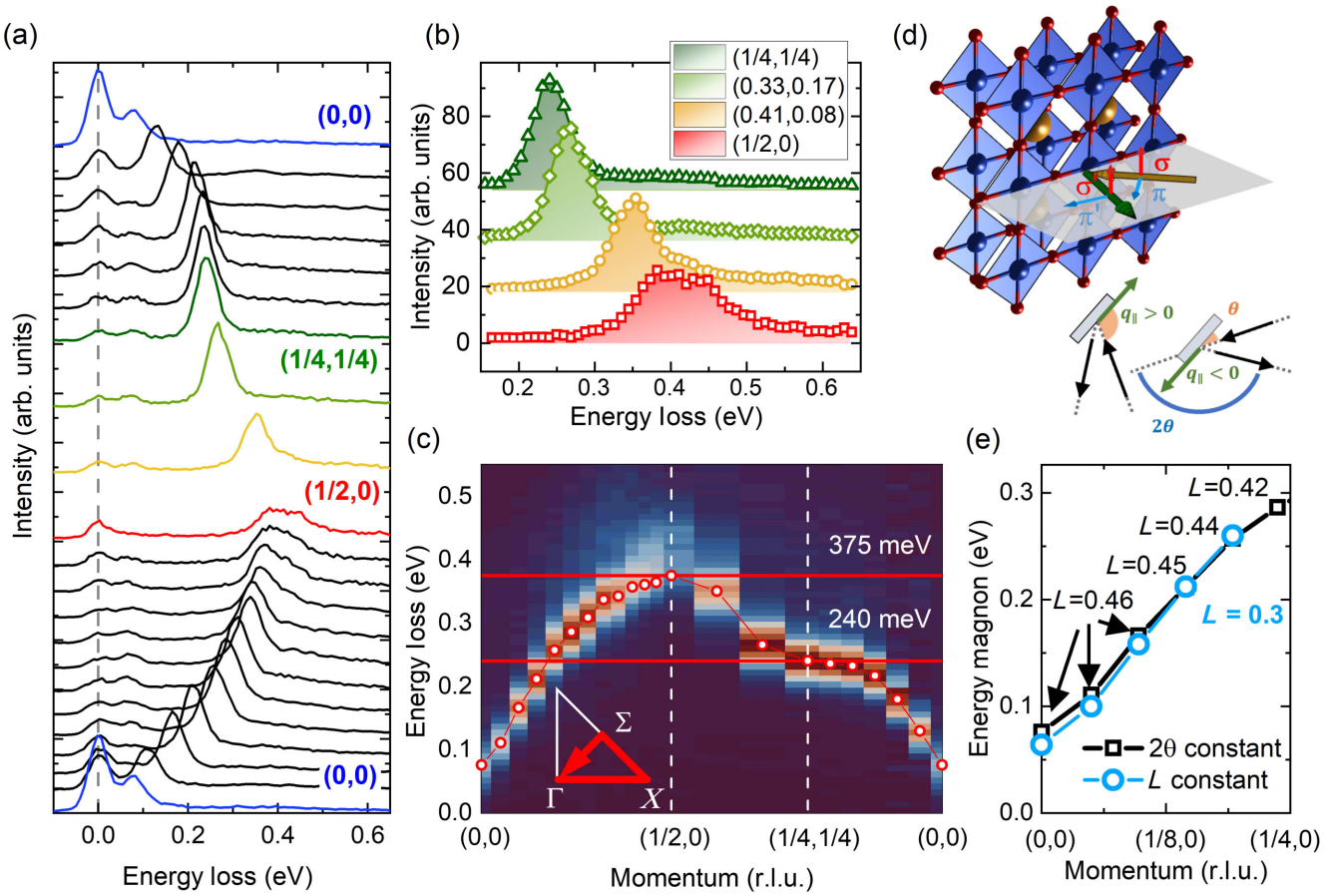

FIG. 2. (a) RIXS scans at different momenta, acquired in grazing-out geometry and π polarization. (b) Evolution of RIXS spectra along the $\Sigma \rightarrow X$ line. Scans have been normalized to the spin-flip cross section. (c) Measured dispersion of the magnon peak along the high-symmetry lines of the Brillouin zone illustrated in the inset. The red dots corresponds to the energy extracted by fitting the experimental data (error bars are smaller than the size of the dots). The two red horizontal lines highlight the magnon energy at (π,0) and at ($\pi/2$,$\pi/2$). (d) Sketch of $CaCuO_2$ crystal structure and experimental geometry used in the RIXS experiments, also showing the incident and outgoing polarization of light. Cu atoms are blue, oxygen atoms are red, and Ca cations are gold. Polarization perpendicular to (lying in the) scattering plane is labeled σ (π). The small inset is a scheme of grazing-in and grazing-out geometries. The shaded orange area represents the incident angle, the scattering angle 2θ is depicted in blue, while the green arrows depict the component of the in-plane transferred momentum. (e) Energy of magnetic excitations along the $\Gamma \rightarrow X$ line measured with constant scattering angle (black squares) and constant L (light blue circles). Note that L values at each point are reported. The incident polarization is π, and we employ grazing-out geometry.

fixed at 149.5°. We indicate the transferred momentum $\mathbf{q}_\parallel$ as (H, K, L) in reciprocal lattice units (r.l.u.), i.e., fractions of the reciprocal lattice vectors $a' = 2\pi/a$, $b' = 2\pi/b$, and $c' = 2\pi/c$. We conventionally assign positive (negative) values of H and K to grazing-out (grazing-in) geometries as depicted in the inset of Fig. 2(d). Moreover, we indicate the high-symmetry in-plane points (0,0), $(1/2, 0)$, and $(1/4, 1/4)$ as Γ, X, and Σ, respectively. We also acquired some scans at a fixed L value, exploiting the continuous rotation of the ERIXS spectrometer to change the angle 2θ [39]. The resolution was about 48 meV unless otherwise indicated. In order to precisely determine the shape of the magnetic excitations, we also collected one high-resolution (~26 meV) spectrum at $(-0.45, 0)$, in a grazing-in configuration and with σ incident polarization. The incident energy was fixed at the resonance peak of the Cu L_3 absorption edge (~931 eV), and the counting time was 30 min for the medium resolution measurements and 5 h for the high-resolution one.

Polarimetric spectra of Sec. III B were acquired at $(+1/2, 0)$ using both σ and π incident polarization with a resolution of 45 meV, better than in previously published measurements [41–43]. Both scans were acquired for 6 h to compensate for the close to 10% efficiency of the polarization analyzer. The error bars were estimated using the formulas given in Ref. [41]. In this geometry, we obtained the parallel- $(\pi\pi', \sigma\sigma')$ and the crossed- $(\pi\sigma', \sigma\pi')$ polarization spectra corresponding to spin-conserving ($\Delta S = 0$) and spin-flip ($\Delta S = 1$) final states, respectively. The former can be assigned to two-magnon excitations, the latter to the

magnon and related fractional continuum and to an odd number of multimagnons. Thus, this type of information is crucial to determine the character of the continuum at the X point.

Detuned RIXS spectra of Sec. III C were acquired at three incident photon energies below the XAS resonant peak ($\Delta E_{\mathrm{in}} = -0.150, -0.450, -0.675$ eV), and performed at the $(-0.43, 0)$ point, i.e., in a grazing-in configuration, with σ incident polarization. In this configuration, we could maximize the count rate and have comparable cross sections for the $\Delta S = 0$ and $\Delta S = 1$ transition channels, and thus distinguish the nature of the various spectral features as being akin to the magnon or the two-magnon. In fact, the intensity scales with the absorption for the former while it falls more rapidly for the latter, as discussed in Refs. [44,45]. Spectra at increasing distance from the resonance peak were acquired for longer times to compensate for the signal decrease, from 30 min to around 2 h. All the measurements were performed at 20 K to minimize radiation damage.

III. EXPERIMENTAL RESULTS

A. Momentum dependence

The scans at different $\mathbf{q}_{\parallel}$ are shown in Fig. 2(a). The π polarization in the grazing-out configuration enhances the magnetic excitations irrespective of the outgoing polarization [46,47]. Below, we often refer to the RIXS intensity in this geometry as purely magnetic; i.e., we assume it is proportional to the dynamical spin susceptibility because the charge response is zero in this energy range in the undoped material, and we neglect the small $\pi\pi'$ spectral contribution. Far from the $(1/2, 0)$ point, a very sharp magnon peak dominates the spectra, on top of a very weak continuum. The energy width of the magnon, correlated with its lifetime, is very small in most of the Brillouin zone and even resolution limited close to the $(1/4, 1/4)$ point. This is due to the absence of doping and to the very high quality of the sample (long-range AF order, little damping by magnetic disorder). A clear reduction in the magnon weight is seen when moving towards the X point. At the same time, another structure extending from the magnon energy up to about 800 meV is evidently increasing in intensity. While this behavior was already observed in cuprates before [6,7,13], we underline that, in the other cuprates, the single magnon is the dominant excitation with respect to the continuum (see, e.g., Ref. [17]). On the contrary, in $CaCuO_2$, the single magnon is submerged by a broad and asymmetric continuum, and it becomes almost undetectable. Figures 2(b) and 2(c) clearly show that this anomalous behavior is restricted to a region of radius about 0.15 r.l.u. around the X point.

As mentioned above, scanning $\mathbf{q}_{\parallel}$ at constant 2θ implies that the out-of-plane component of the transferred momentum changes, too. In particular, L ranges from about 0.46 to about 0.22 when moving from (0,0) to (0.5,0). Since CCO is known to possess a more three-dimensional magnetic structure as compared to the other cuprates—implying a nonzero energy of the magnon at $(0, 0, L)$ with a noninteger value of L [7,48]—we also acquired some RIXS spectra along a limited range of the same in-plane path but at constant $L = 0.3$. While the magnon energy is different at the Γ point, the difference decreases at larger in-plane

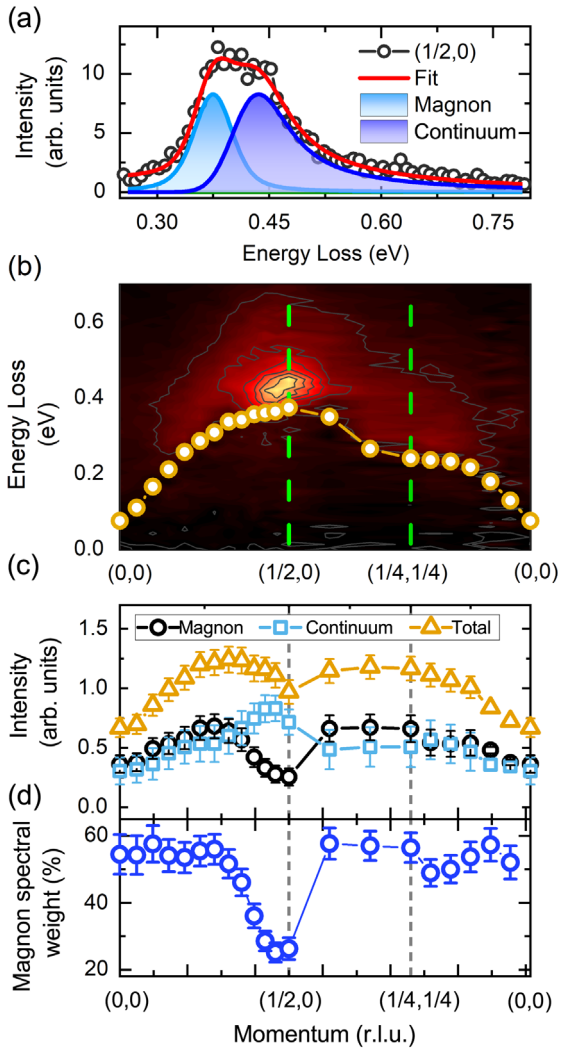

FIG. 3. (a) Example of fitting procedure of the spectrum at (0.5,0) collected with π polarization. The magnon peak and the continuum are reported in light and deep blue, respectively, and the resulting fitted curve is in red. (b) Momentum dependence of high-energy continuum. Elastic, phonon, and magnon peaks have been removed for clarity. The energy of the magnon is shown by yellow dots. For clarity, the scans have been normalized to the atomic $\pi\sigma'$ RIXS cross section, which slightly modulates the intensity but only depends on experimental geometry [46]. (c) Intensity (determined as the area below the curves) of the magnon, of the continuum, and of the total of the magnetic excitations as a function of momentum. (d) Ratio between the weight of the magnon peak and the total weight of the magnetic excitations.

momenta and vanishes for $H > 1/8$, as shown in Fig. 2(d). We thus assume that the anomaly at the X point is negligibly influenced by the value of L.

The false-color map of Fig. 2(c) shows the RIXS intensity along the in-plane momentum path depicted in the inset, with the energy of the single magnon marked by the red dots. The large energy $E_X \approx 375$ meV at $(1/2, 0)$ and the strong dispersion along the magnetic zone boundary ($\Delta E_{\mathrm{MZB}} = E_X - E_\Sigma \approx 135$ meV) are signatures of the fact that J_1 and J_c are both very large, probably the largest among all layered cuprates [7,49].

As the magnon dispersion was previously analyzed in detail [7], we concentrate here on the anomaly at the X point, with the aim of determining if the single magnon that dominates everywhere else is replaced here by multiples or by fractions of magnons. To extract the exact momentum-dependent intensity of this continuum, we fit the spectra in the [0, 0.8] eV energy range as depicted in Fig. 3(a): a Gaussian shape for the elastic or quasielastic and phonon peaks (assumed to be resolution limited), a Voigt profile for the single magnon (whose intrinsic linewidth might not be negligible), and an asymmetric Lorentzian profile (like the one described in Ref. [50]) for the high-energy continuum above it. Spectral weights have been taken as the area below the curves. In Fig. 3(b), we plot the intensity map along the $\Gamma - X - \Sigma - \Gamma$ line after removal of the elastic, phonon, and single-magnon contributions; the energy of the magnon is indicated by the yellow dots.

The fitting procedure of our RIXS spectra allows us to quantify the single magnon and the continuum spectral weights as a function of momentum transfer; the results are shown in Fig. 3(c). The intensities have been normalized to the RIXS spin-flip cross section, only dependent on the experimental geometry; this is justified since the spectral weight predominantly comes from the $\Delta S = 1$ excitations in this geometry. Evidently, the total weight of magnetic excitations partially decreases close to the zone boundary, but the single-magnon intensity drops more sharply and is, for the most part, transferred to the high-energy continuum. Incidentally, we note that the spectral weight close to Γ is small but not zero because of the three-dimensional character of magnetic excitations in CCO [7]. However, this has a negligible effect on the physics close to the zone boundary, as we thoroughly discuss in the Appendix. Figure 3(d) displays the ratio between the weight of the single magnon and the total sum of the magnetic excitations (which is relevant since it is independent of the normalization to the RIXS cross section). Away from the $(1/2, 0)$ point, the single-magnon contribution is rather constant and constitutes roughly 60% of the total RIXS intensity; this value drops by a factor of 3 to about 20% at the X point. This deviation seems to be confined within 0.15 r.l.u. around X.

The anomalous shape of the magnetic spectrum close to the X point might be seen as a strongly damped (i.e., intrinsically broad) magnon [50–52], possibly combined with a "local" bimagnon excitation of comparable intensity [34,47]. To check for the amount of bimagnon contribution to the continuum, we perform measurements with σ-polarized incident photons and a grazing-in geometry (negative H), for which the single-ion cross sections predict appreciable intensity for both $\sigma\sigma'$ and $\sigma\pi'$ channels [46], i.e., the $\Delta S = 0$ (even-order multiple-magnon) and $\Delta S = 1$ (single-magnon) contributions, respectively. We exploit the best-available energy resolution at the beam line (26 meV) to define, as precisely as possible, the intrinsic shape of the magnetic spectrum at the $(-0.45, 0)$ point, where the magnon peak is still discernible while a sizable continuum is already visible. The spectrum of Fig. 4(a) shows that the high-energy continuum is not the tail of a broad magnon but rather an independent, well-defined spectral feature. Fitting the spectrum, we obtain an almost

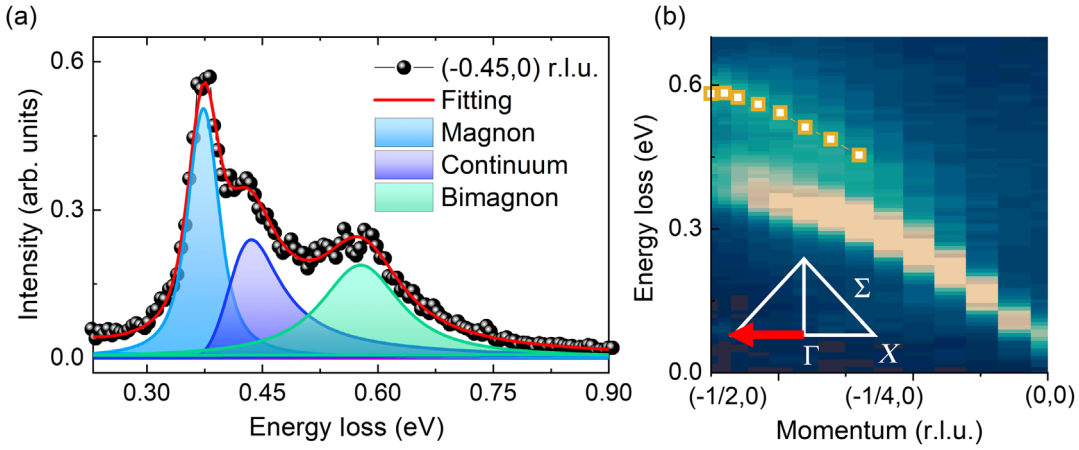

FIG. 4. (a) High-resolution (approximately 26.3 meV) spectra acquired at $(-0.45,0)$ using σ polarization. The use of high resolution clearly allows us to disentangle the single-magnon peak and the bimagnon peak from the high-energy tail. (b) Map of RIXS spectra along the $\Gamma \rightarrow (-X)$ line, acquired with σ incident polarization and grazing-in geometry. Momentum values are reported with positive signs for clarity. The energy of bimagnon excitations extracted with a fitting is highlighted in yellow squares.

resolution-limited magnon at 340 meV and a satellite peaked at 440 meV with a width of 33 ± 5 meV. The use of σ polarization also allows us to detect a well-defined feature around 540 meV, whose incident-energy and polarization dependence (see below) identify it as a local bimagnon [46,47]. The momentum dependence along the $\Gamma \rightarrow X$ line shown in Fig. 4(b) confirms that this feature is more intense closer to X and disperses upward as predicted by calculations for bimagnons [13,47]. We can therefore exclude the idea that the continuum closer to the magnon peak is a local bimagnon. This implies that, also in the spectra measured with π polarization at positive H—a configuration that minimizes the even multiple-magnon contribution—the continuum is not due to local bimagnons.

B. Polarimetric measurements

We have shown that the continuum is not due to the relatively sharp bimagnon observed, for example, in $S_2CuO_2Cl_2$ (SCOC) [17], but this does not rule out the idea that it might be due to other types of spin-conserving excitations, i.e., an incoherent continuum of two magnons. To truly determine its nature, we perform RIXS measurements with polarization analysis on the scattered beam [39–41]. By disentangling the vertical and horizontal polarization components of the scattered x rays, we are able to separate the crossed and parallel channels, corresponding to excitations with $\Delta S = 1$ and $\Delta S = 0$, respectively. Indeed, although significant, the distinction of the two channels based on the incident photon polarization and on the RIXS cross sections in the single-ion model is not always conclusive. In fact, it was demonstrated that for SCOC nonlocal scattering, operators have to be introduced to fully account for the RIXS spectral shape close to the X point [17].

For convenience, in Fig. 5, we present the complete set of polarization-resolved spectra of CCO and SCOC measured at the X point. In both samples, the π spectra are dominated by the crossed polarization components (red symbols), but, whereas the parallel (blue) contribution is non-negligible in SCOC, it is practically zero everywhere in CCO. Therefore, the high-energy satellite of the magnon of CCO also clearly belongs to the $\Delta S = 1$ channel. On the contrary, when exciting with σ polarization, the spectra are predominantly of parallel character (blue) in CCO and of mixed character in SCOC. Hence, the relatively sharp peak around 540 meV $\approx 3J$, clearly resolved in the high-resolution spectra of CCO, can be regarded as a local bimagnon excitation. Interestingly, in the large-J_c CCO, we observe no signature of the complex multimagnon dynamics emerging in the small-J_c SCOC [17].

C. Energy dependence of the magnon and continuum

To further investigate the nature of the magnetic excitations, we acquire RIXS measurements at different incident photon energies (so-called "detuning" analysis). Figure 6 depicts some RIXS scans at selected incident

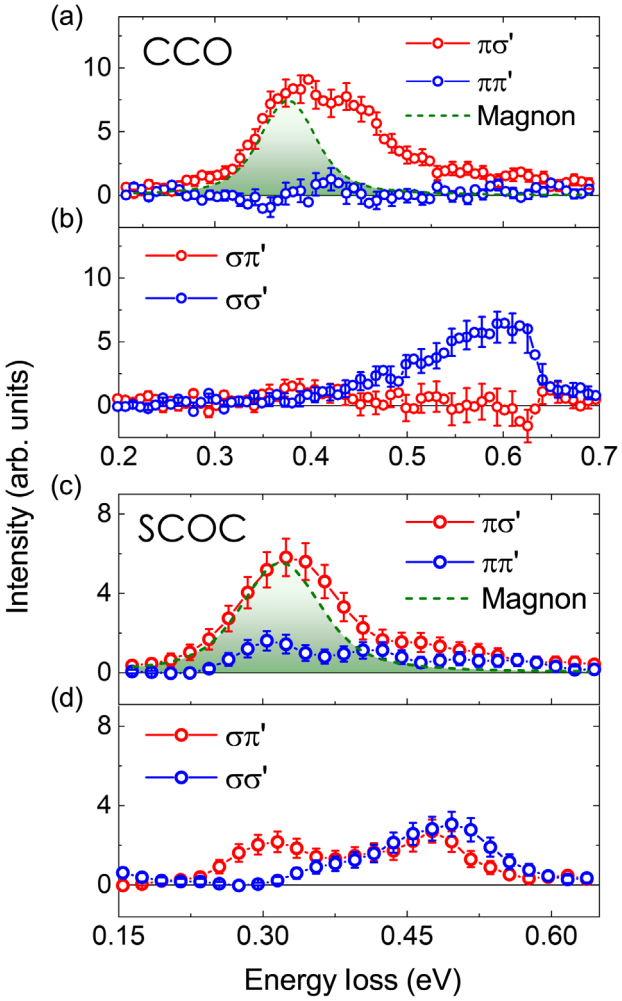

FIG. 5. Polarimetric spectra collected at $(1/2, 0)$ for CCO [panels (a) and (b)] and SCOC [(c) and (d)]. Panels (a) and (c) show the spectra acquired at $(+1/2,0)$ with incident π polarization, while panels (b) and (d) show the spectra measured with incident σ polarization to maximize the signal coming from non-spin-flip excitations. Blue curves always denote the parallel channel, while red ones show the crossed channel. Note that the resolution of the SCOC data is worse (approximately 65 meV) [17], so the line shape appears to be broader.

energies. The sharp, intense peak at about 80 meV is a bond-stretching phonon excitation [48], which can also be identified in the scans in Fig. 2 but is more visible here because of the favorable scattering geometry. By fitting the spectra in the way described in Sec. III, we estimate the relative weights of the magnon, the continuum, and the bimagnon excitations. By comparing their incident-energy dependence to the XAS profile (see inset), we observe that the $\Delta S = 1$ structure above 400 meV shares the same energy dependence of the single magnon and of the XAS, as opposed to the bimagnon intensity that decreases faster upon detuning, as previously observed [44,45,53]. This is further evidence that the continuum gets excited via the same process as the magnon and that its

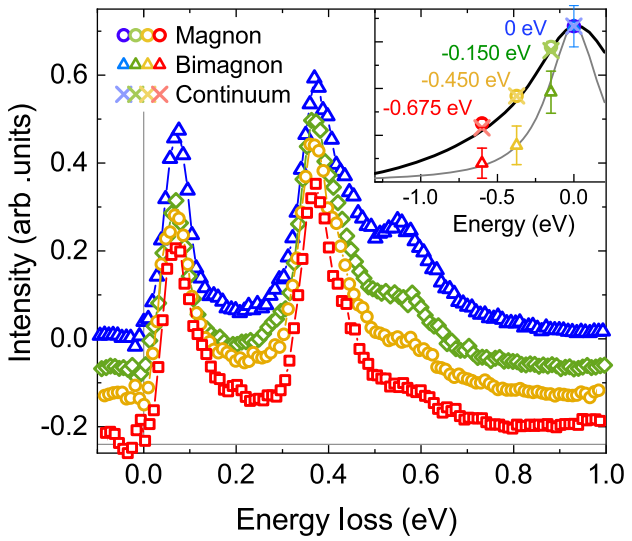

FIG. 6. Inelastic RIXS spectra at different incident energies. The elastic line has been removed for clarity. All the spectra are acquired at (−0.43,0) using σ polarization, in order to have appreciable intensity for both the magnon and bimagnon signals. The scans have also been normalized to the value of the XAS. The inset shows the XAS signal (solid black line), the intensity of the magnon peak (circles), of the continuum (crosses) and of the bimagnon (triangles). The gray solid line is a guide to the eye. All intensities have been normalized to the resonance value, and the energies are referred to the maximum of the XAS (931.6 eV). The errors on the intensity of the continuum and the magnon are of the size of the symbols.

intensity is not related to the lifetime of the RIXS intermediate state, which is not the case for the bimagnon.

IV. DISCUSSION

We have found strong experimental evidence that the continuum appearing in the RIXS spectra when approaching the X point has $\Delta S = 1$ character and is thus compatible with being the decay of magnons into spinon pairs [11,20,22,32]. As fractional excitations in spin-1/2 square lattices have been predicted in several Heisenberg-like Hamiltonians [11,19,20,22,29–31,33], spinon pairs have often been invoked to explain the anomalous high-energy dynamics of cuprates [10] and isostructural iridates [12]. However, undisputed experimental evidence of their existence in 2D is still missing. It is important to highlight that spinon pairs are also predicted in the presence of Néel antiferromagnetic order in the square lattice. Indeed, calculations predict that the proximity of the Néel phase to some exotic magnetic phase gives rise to a broad, gapped spinon band above the magnon energy, dispersing as [19,23,32,54]

$$E(H,K) \approx \sqrt{E_0^2 - (E_1 \cos(2\pi H)\cos(2\pi K))^2}. \quad (1)$$

The spinon pair dispersion reaches a maximum at $(1/4, 1/4)$ and a minimum at $(1/2, 0)$. Here, where the magnons reach their maximum energy, the mixing of spinon pairs with magnons becomes possible. The transfer of spectral weight is made possible by the quasidegeneracy in energy and by the common $\Delta S = 1$ nature of magnons and spinon pairs [55]. It is important to note that two-spinon excitation dispersion in 1D spin systems has been observed by RIXS [42,56]. In interpreting the data, we have used the fact that the RIXS spectral function for the spin-flip channel (where our interest lies) is, in spin-1/2 AF cuprates, approximately proportional to the dynamical structure factor usually measured in neutron scattering. This correspondence is well established, having received strong experimental [17,42,51,56,57] and theoretical [58–60] confirmation in recent years.

To understand why the X-point anomaly in the magnetic spectrum is larger in CCO than in other cuprates, we look at the magnetic exchange constants. We consider the usual spin Hamiltonian, which can also be obtained as a fourth-order expansion of the one-band Hubbard model [6,28,61,62], based on the definitions of Fig. 1(a),

$$\begin{aligned} H = {} & J_1 \sum_{ii'} \mathbf{S}_i \cdot \mathbf{S}_{i'} + J_2 \sum_{ii''} \mathbf{S}_i \cdot \mathbf{S}_{i''} + J_3 \sum_{ii'''} \mathbf{S}_i \cdot \mathbf{S}_{i'''} \\ & + J_c \sum_{\langle ijkl \rangle} (\mathbf{S}_i \cdot \mathbf{S}_j)(\mathbf{S}_k \cdot \mathbf{S}_l) + (\mathbf{S}_i \cdot \mathbf{S}_l)(\mathbf{S}_k \cdot \mathbf{S}_j) \\ & - (\mathbf{S}_i \cdot \mathbf{S}_k)(\mathbf{S}_j \cdot \mathbf{S}_l). \end{aligned} \quad (2)$$

A simple analytical calculation relates the magnon energy at $(1/2, 0)$ and $(1/4, 1/4)$ and the values of J_1 and J_c [6,61]:

$$\frac{J_1}{J_c} = \frac{3}{10} \frac{1 + \Delta E_{\mathrm{MZB}}/E_X}{\Delta E_{\mathrm{MZB}}/E_X}. \quad (3)$$

In the case of CCO, with the values extracted from Fig. 2(c), Eq. (3) translates in $J_c \approx J_1$. This value of J_c/J_1 is the largest among cuprates: For example, in the $RBa_2Cu_3O_6$ family, this ratio is 0.8; in La_2CuO_4, about 0.29; in single-layer $Bi_2Sr_2CuO_6$, about 0.62 [7]; and in $Sr_2CuO_2Cl_2$, about 0.42 [17,49]. A ratio J_c/J close to 1 is also confirmed by a global fitting of the experimental dispersion using the Hamiltonian (2) in a LSWT approach, which yields $J = 172 \pm 7$ meV and $J_c = 167 \pm 20$ (and $J_\perp = 7 \pm 3$ meV for the small interlayer coupling), giving $J_c/J \approx 0.97$. We note, incidentally, that the values of J_c and J_1 determined here are slightly different from the ones reported in Ref. [7]: The increased resolution allowed us to determine the shape of the spectrum more precisely and to correctly identify the position of the single magnon even close to $(1/2, 0)$.

It is therefore natural to correlate the high-energy continuum, which we interpret as being made of fractionalized magnetic excitations, to the strong J_c, which, in this material, cannot be regarded as a small perturbation. The presence of spinons in the spectrum of the Heisenberg AF with strong multispin couplings (of which the ring exchange is an example) was predicted some years ago and is now well established [20–22,33]. Interestingly, a recent exact diagonalization study [63] performed on the

EHM Hamiltonian has shown that, at $J_c/J \approx 1$, the excitation spectrum at $(1/2, 0)$ breaks into a continuum of states very close in energy, similarly to what has been calculated for Néel-RVB and Néel-VBS transitions [20,29–32].

V. CONCLUSIONS

We have performed a deep investigation of the magnetic excitations in the infinite-layer cuprate $CaCuO_2$ using RIXS, analyzing their dependence on momentum, incident and outgoing polarization, and incident energy. The momentum dependence reveals a clear anomaly, close to the X point in reciprocal space, which is clearly not explainable in terms of a simple magnon with increased width. The incident polarization dependence rules out that this anomaly can be due to local bimagnon excitations. Conversely, its interpretation in terms of a continuum of spinon pairs is strongly supported both by the polarimetric analysis and by the incident-energy dependence, which clearly shows that this anomalous scattering channel originates from a direct RIXS process. A deviation from the LSWT scenario is a general property of all square-lattice AF materials, even of systems where the nearest-neighbor coupling is the only dominant interaction [2]. However, the measured continuum is greatly enhanced in this material even with respect to other cuprates, and at the same time, the multimagnon features seem to be suppressed. An estimate of the next-nearest-neighbor magnetic interactions suggests that the cause of these peculiarities lies in the exceptionally large value of ring exchange coupling J_c and, in general, in large values of the superexchange integrals, rooted in the absence of the hole-localizing potential provided by the apical oxygens [7]. It would therefore be of interest to perform the same experimental investigation on Nd_2CuO_4, in which the absence of "direct" apical oxygens [64] should enhance the ring exchange [7], similarly to what happens in CCO.

In conclusion, here we provide the experimental evidence of fractional spin excitations in the magnetic spectrum of a layered cuprate. Spinon pairs are a well-established feature of 1D magnetic systems and were predicted by different theoretical approaches to also be present in 2D AF lattices [19–22,32]. However, their observation in layered cuprates had remained somehow inconclusive so far [10], and our results can support the assignment of the magnon anomaly close to the X point to fractional spin excitations also in other cuprates. More in general, we demonstrate that multispin couplings play a nonmarginal role in determining the short-wavelength physics of the magnetic excitations, as indeed proposed by several theories [14,21,63].

ACKNOWLEDGMENTS

We acknowledge José Lorenzana for enlightening discussions. The RIXS experimental data were collected at beamline ID32 of the European Synchrotron (ESRF) in Grenoble, France, using the ERIXS spectrometer designed jointly by the ESRF and Politecnico di Milano. M. M. S. and G. G. acknowledge support by the project PRIN2017 Quantum-2D ID 2017Z8TS5B of the Ministry for University and Research (MIUR) of Italy. R. A. acknowledges support by the Swedish Research Council (VR) under Project No. 2020-04945.

APPENDIX: LINEAR SPIN-WAVE FITTING OF EXPERIMENTAL DATA

In order to estimate the values of J_1, J_c, and $J_\perp$, we have performed a fit of the single-magnon dispersion using the software spinW [65], which solves the magnetic Hamiltonian using a LSWT approach. The direction of the magnetic moments of Cu atoms has been set along the [110] direction like for all other cuprates [2,11,61]. The quantum renormalization factor Z_c has been set to 1.18, again following the literature [2,6,10,11]. The result of the fitting is displayed in Fig. 7(a). We obtain $J = 172 \pm 7$ meV, $J_c = 167 \pm 20$ meV, and $J_\perp = 7 \pm 3$ meV. As stated in Sec. IV, these values are slightly different from the ones reported in Ref. [7]: This is because of a better estimation of the real

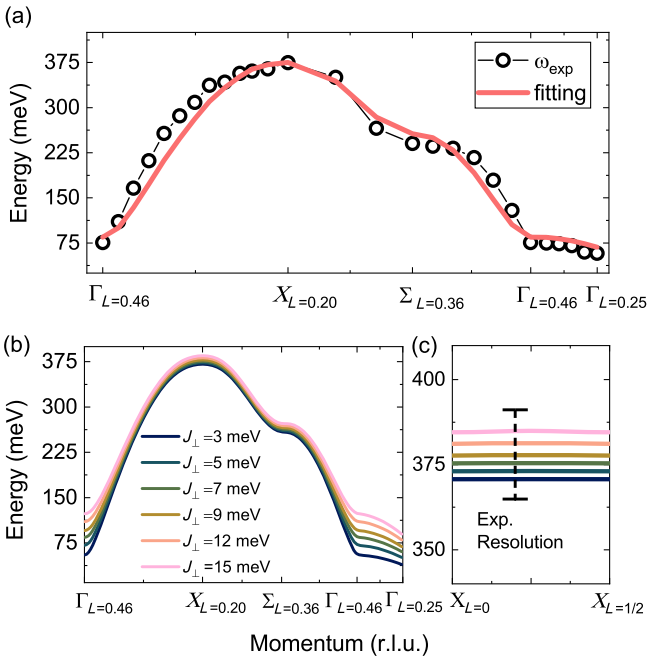

FIG. 7. Summary of fitting and simulations done with the spinW software. (a) Fitting of the experimental dispersion. The (H, K) coordinates of the measured momenta are indicated by their letter as described in Sec. II, while the subscripts indicate the L value. The paths between $\Gamma_{L=0.46}, X_{L=0.20}, \Sigma_{L=0.36}, \Gamma_{L=0.46}$ are circumference arcs in the H–L plane, while the last segment is a straight line. (b) Calculated dispersion along the same path for different $J_\perp$ values. (c) Calculated L dependence at the X point for the same $J_\perp$ values as in panel (b). The black dotted line is our best experimental resolution (26 meV).

single-magnon energy close to the X point, possible thanks to an improved experimental resolution (around 42 meV in our work, 55 meV in Ref. [7]). We also underline that the value of J_c/J obtained from the global fitting is approximately 0.97, very similar to the one calculated in Eq. (3), just considering the dispersion along the magnetic zone boundary. The value of $J_\perp$ is also consistent with what has been extracted from neutron scattering measurements in $YBa_2Cu_3O_{6+x}$ [66,67]: This is expected since the distance between the two CuO_2 layers in the YBCO unit cell is the same as in CCO. We therefore obtain $J_1/J_\perp \approx 25$. To verify that, at least in a LWST approach, the physics of the material close to the magnetic zone boundary is effectively two dimensional, we have also performed other simulations again using the spinW software. First, we have calculated the magnon dispersion by letting $J_\perp$ change in a reasonable range between 3 and 15 meV. The results are shown in Fig. 7(b): Evidently, the only appreciable effects of $J_\perp$ are visible very close to Γ, while the differences of the curves close to the zone boundary are well below our best experimental resolution (26 meV). Additionally, we have verified that the energy of the single magnon is not affected by changes in L close to the X point by calculating the energy of the single magnon along the $(1/2, 0, 0) \rightarrow (1/2, 0, 1/2)$ line. Each curve shows a dispersion of less than 1 meV (not visible in the figure). This further demonstrates that the magnetic physics close to the zone boundary is effectively two dimensional.

[1] Bernhard Keimer, Steven A. Kivelson, Michael R. Norman, Shinichi Uchida, and J. Zaanen, *From Quantum Matter to High-Temperature Superconductivity in Copper Oxides*, Nature (London) **518**, 179 (2015).

[2] Niels Bech Christensen, Henrik Moodysson Rønnow, Desmond Francis McMorrow, A. Harrison, T. G. Perring, Mechtild Enderle, R. Coldea, L. P. Regnault, and G. Aeppli, *Quantum Dynamics and Entanglement of Spins on a Square Lattice*, Proc. Natl. Acad. Sci. U.S.A. **104**, 15264 (2007).

[3] D. Vaknin, S. K. Sinha, D. E. Moncton, D. C. Johnston, J. M. Newsam, C. R. Safinya, and H. E. King, *Antiferromagnetism in* La_2CuO_{4-y}, Phys. Rev. Lett. **58**, 2802 (1987).

[4] Y. Endoh, K. Yamada, R. J. Birgeneau, D. R. Gabbe, H. P. Jenssen, M. A. Kastner, C. J. Peters, P. J. Picone, T. R. Thurston, J. M. Tranquada, G. Shirane, Y. Hidaka, M. Oda, Y. Enomoto, M. Suzuki, and T. Murakami, *Static and Dynamic Spin Correlations in Pure and Doped* La_2CuO_4, Phys. Rev. B **37**, 7443 (1988).

[5] G. Aeppli, S. M. Hayden, H. A. Mook, Z. Fisk, S.-W. Cheong, D. Rytz, J. P. Remeika, G. P. Espinosa, and A. S. Cooper, *Magnetic Dynamics of* La_2CuO_4 *and* $La_{2-x}Ba_xCuO_4$, Phys. Rev. Lett. **62**, 2052 (1989).

[6] R. Coldea, S. M. Hayden, G. Aeppli, T. G. Perring, C. D. Frost, T. E. Mason, S.-W. Cheong, and Z. Fisk, *Spin Waves and Electronic Interactions in* La_2CuO_4, Phys. Rev. Lett. **86**, 5377 (2001).

[7] Y. Y. Peng, G. Dellea, M. Minola, M. Conni, A. Amorese, D. Di Castro, G. M. De Luca, K. Kummer, M. Salluzzo, X. Sun *et al.*, *Influence of Apical Oxygen on the Extent of In-Plane Exchange Interaction in Cuprate Superconductors*, Nat. Phys. **13**, 1201 (2017).

[8] Sudip Chakravarty, Bertrand I. Halperin, and David R. Nelson, *Two-Dimensional Quantum Heisenberg Antiferromagnet at Low Temperatures*, Phys. Rev. B **39**, 2344 (1989).

[9] Kingshuk Majumdar, Douglas Furton, and Götz S. Uhrig, *Effects of Ring Exchange Interaction on the Néel Phase of Two-Dimensional, Spatially Anisotropic, Frustrated Heisenberg Quantum Antiferromagnet*, Phys. Rev. B **85**, 144420 (2012).

[10] N. S. Headings, S. M. Hayden, R. Coldea, and T. G. Perring, *Anomalous High-Energy Spin Excitations in the High-*T_c *Superconductor-Parent Antiferromagnet* La_2CuO_4, Phys. Rev. Lett. **105**, 247001 (2010).

[11] Bastien Dalla Piazza, M. Mourigal, Niels Bech Christensen, G. J. Nilsen, P. Tregenna-Piggott, T. G. Perring, Mechtild Enderle, Desmond Francis McMorrow, D. A. Ivanov, and Henrik Moodysson Rønnow, *Fractional Excitations in the Square-Lattice Quantum Antiferromagnet*, Nat. Phys. **11**, 62 (2015).

[12] H. Gretarsson, N. H. Sung, J. Porras, J. Bertinshaw, C. Dietl, Jan A. N. Bruin, A. F. Bangura, Y. K. Kim, R. Dinnebier, Jungho Kim, A. Al-Zein, M. Moretti Sala, M. Krisch, M. Le Tacon, B. Keimer, and B. J. Kim, *Persistent Paramagnons Deep in the Metallic Phase of* $Sr_{2-x}La_xIrO_4$, Phys. Rev. Lett. **117**, 107001 (2016).

[13] Jun-ichi Igarashi and Tatsuya Nagao, *Magnetic Excitations in L-Edge Resonant Inelastic X-Ray Scattering from Cuprate Compounds*, Phys. Rev. B **85**, 064421 (2012).

[14] Anders W. Sandvik and Rajiv R. P. Singh, *High-Energy Magnon Dispersion and Multimagnon Continuum in the Two-Dimensional Heisenberg Antiferromagnet*, Phys. Rev. Lett. **86**, 528 (2001).

[15] J. Lorenzana, J. Eroles, and S. Sorella, *Does the Heisenberg Model Describe the Multimagnon Spin Dynamics in Antiferromagnetic CuO Layers?*, Phys. Rev. Lett. **83**, 5122 (1999).

[16] M. Powalski, K. P. Schmidt, and G. S. Uhrig, *Mutually Attracting Spin Waves in the Square-Lattice Quantum Antiferromagnet*, SciPost Phys. **4**, 001 (2018).

[17] Davide Betto, Roberto Fumagalli, Leonardo Martinelli, Matteo Rossi, Riccardo Piombo, Kazuyoshi Yoshimi, Daniele Di Castro, Emiliano Di Gennaro, Alessia Sambri, Doug Bonn, George A. Sawatzky, Lucio Braicovich, Nicholas B. Brookes, Jos Lorenzana, and Giacomo Ghiringhelli, *Multiple-Magnon Excitations Shape the Spin Spectrum of Cuprate Parent Compounds*, Phys. Rev. B **103**, L140409 (2021).

[18] Philip W. Anderson, *The Resonating Valence Bond State in* La_2CuO_4 *and Superconductivity*, Science **235**, 1196 (1987).

[19] Chang-Ming Ho, V. N. Muthukumar, Masao Ogata, and P. W. Anderson, *Nature of Spin Excitations in Two-Dimensional Mott Insulators: Undoped Cuprates and Other Materials*, Phys. Rev. Lett. **86**, 1626 (2001).

[20] Anders W. Sandvik, *Evidence for Deconfined Quantum Criticality in a Two-Dimensional Heisenberg Model with Four-Spin Interactions*, Phys. Rev. Lett. **98**, 227202 (2007).

[21] Ying Tang and Anders W. Sandvik, *Confinement and Deconfinement of Spinons in Two Dimensions*, Phys. Rev. Lett. **110**, 217213 (2013).

[22] Hui Shao, Yan Qi Qin, Sylvain Capponi, Stefano Chesi, Zi Yang Meng, and Anders W. Sandvik, *Nearly Deconfined Spinon Excitations in the Square-Lattice Spin-1/2 Heisenberg Antiferromagnet*, Phys. Rev. X **7**, 041072 (2017).

[23] J. M. P. Carmelo, M. A. N. Araújo, S. R. White, and M. J. Sampaio, *Hubbard-Model Description of the High-Energy Spin-Weight Distribution in* La_2CuO_4, Phys. Rev. B **86**, 064520 (2012).

[24] F. C. Zhang and T. M. Rice, *Effective Hamiltonian for the Superconducting Cu Oxides*, Phys. Rev. B **37**, 3759 (1988).

[25] Akihiro Ino, Changyoung Kim, Takashi Mizokawa, Zhi-Xun Shen, Atsushi Fujimori, Masamitsu Takaba, Kenji Tamasaku, Hiroshi Eisaki, and Shinichi Uchida, *Fermi Surface and Band Dispersion in* $La_{2-x}Sr_xCuO_4$, J. Phys. Soc. Jpn. **68**, 1496 (1999).

[26] Andrea Damascelli, Zahid Hussain, and Zhi-Xun Shen, *Angle-Resolved Photoemission Studies of the Cuprate Superconductors*, Rev. Mod. Phys. **75**, 473 (2003).

[27] T. Yoshida, X. J. Zhou, K. Tanaka, W. L. Yang, Z. Hussain, Z.-X. Shen, A. Fujimori, S. Sahrakorpi, M. Lindroos, R. S. Markiewicz, A. Bansil, Seiki Komiya, Yoichi Ando, H. Eisaki, T. Kakeshita, and S. Uchida, *Systematic Doping Evolution of the Underlying Fermi Surface of* $La_{2-x}Sr_xCuO_4$, Phys. Rev. B **74**, 224510 (2006).

[28] N. M. R. Peres and M. A. N. Araújo, *Spin-Wave Dispersion in* La_2CuO_4, Phys. Rev. B **65**, 132404 (2002).

[29] H. J. Schulz, T. A. L. Ziman, and Didier Poilblanc, *Magnetic Order and Disorder in the Frustrated Quantum Heisenberg Antiferromagnet in Two Dimensions*, J. Phys. I **6**, 675 (1996).

[30] L. Isaev, G. Ortiz, and J. Dukelsky, *Hierarchical Mean-Field Approach to the* $J_1 - J_2$ *Heisenberg Model on a Square Lattice*, Phys. Rev. B **79**, 024409 (2009).

[31] Luca Capriotti, Federico Becca, Alberto Parola, and Sandro Sorella, *Resonating Valence Bond Wave Functions for Strongly Frustrated Spin Systems*, Phys. Rev. Lett. **87**, 097201 (2001).

[32] Francesco Ferrari and Federico Becca, *Spectral Signatures of Fractionalization in the Frustrated Heisenberg Model on the Square Lattice*, Phys. Rev. B **98**, 100405(R) (2018).

[33] Jun Takahashi and Anders W. Sandvik, *Valence-Bond Solids, Vestigial Order, and Emergent SO(5) Symmetry in a Two-Dimensional Quantum Magnet*, Phys. Rev. Research **2**, 033459 (2020).

[34] Lucio Braicovich, L. J. P. Ament, Valentina Bisogni, F. Forte, C. Aruta, G. Balestrino, N. B. Brookes, G. M. De Luca, P. G. Medaglia, F. Miletto Granozio *et al.*, *Dispersion of Magnetic Excitations in the Cuprate* La_2CuO_4 *and* $CaCuO_2$ *Compounds Measured Using Resonant X-Ray Scattering*, Phys. Rev. Lett. **102**, 167401 (2009).

[35] H. Zhang, Y. Y. Wang, H. Zhang, V. P. Dravid, L. D. Marks, P. D. Han, D. A. Payne, P. G. Radaelli, and J. D. Jorgensen, *Identity of Planar Defects in the 'Infinite-Layer' Copper Oxide Superconductor*, Nature (London) **370**, 352 (1994).

[36] D. Di Castro, C. Cantoni, F. Ridolfi, C. Aruta, A. Tebano, N. Yang, and G. Balestrino, *High-*T_c *Superconductivity at the Interface between the* $CaCuO_2$ *and* $SrTiO_3$ *Insulating Oxides*, Phys. Rev. Lett. **115**, 147001 (2015).

[37] D. Di Castro, C. Aruta, A. Tebano, D. Innocenti, M. Minola, M. Moretti Sala, W. Prellier, O. Lebedev, and G. Balestrino, T_c *up to 50 K in Superlattices of Insulating Oxides*, Supercond. Sci. Technol. **27**, 044016 (2014).

[38] D. Di Castro, M. Salvato, A. Tebano, D. Innocenti, C. Aruta, W. Prellier, O. I. Lebedev, I. Ottaviani, N. B. Brookes, M. Minola, M. Moretti Sala, C. Mazzoli, P. G. Medaglia, G. Ghiringhelli, L. Braicovich, M. Cirillo, and G. Balestrino, *Occurrence of a High-Temperature Superconducting Phase in* $((CaCuO_2)_n/(SrTiO_3)_m$ *Superlattices*, Phys. Rev. B **86**, 134524 (2012).

[39] N. B. Brookes, F. Yakhou-Harris, K. Kummer, A. Fondacaro, J. C. Cezar, D. Betto, E. Velez-Fort, A. Amorese, G. Ghiringhelli, L. Braicovich, R. Barrett, G. Berruyer, F. Cianciosi, L. Eybert, P. Marion, P. van der Linden, and L. Zhang, *The Beamline ID32 at the ESRF for Soft X-Ray High Energy Resolution Resonant Inelastic X-Ray Scattering and Polarisation Dependent X-Ray Absorption Spectroscopy*, Nucl. Instrum. Methods Phys. Res., Sect. A **903**, 175 (2018).

[40] Lucio Braicovich, Matteo Minola, Greta Dellea, M. Le Tacon, M. Moretti Sala, C. Morawe, J.-Ch. Peffen, R. Supruangnet, F. Yakhou, G. Ghiringhelli *et al.*, *The Simultaneous Measurement of Energy and Linear Polarization of the Scattered Radiation in Resonant Inelastic Soft X-Ray Scattering*, Rev. Sci. Instrum. **85**, 115104 (2014).

[41] R. Fumagalli, L. Braicovich, M. Minola, Y. Y. Peng, K. Kummer, D. Betto, M. Rossi, E. Lefrançois, C. Morawe, M. Salluzzo, H. Suzuki, F. Yakhou, M. Le Tacon, B. Keimer, N. B. Brookes, M. Moretti Sala, and G. Ghiringhelli, *Polarization-Resolved Cu* L_3*-edge Resonant Inelastic X-Ray Scattering of Orbital and Spin Excitations in* $NdBa_2Cu_3O_{7-\delta}$, Phys. Rev. B **99**, 134517 (2019).

[42] R. Fumagalli, J. Heverhagen, D. Betto, R. Arpaia, M. Rossi, D. Di Castro, N. B. Brookes, M. Moretti Sala, M. Daghofer, L. Braicovich, K. Wohlfeld, and G. Ghiringhelli, *Mobile Orbitons in* Ca_2CuO_3*: Crucial Role of Hund's Exchange*, Phys. Rev. B **101**, 205117 (2020).

[43] Matthias Hepting, Laura Chaix, E. W. Huang, R. Fumagalli, Y. Y. Peng, B. Moritz, K. Kummer, N. B. Brookes, W. C. Lee, M. Hashimoto *et al.*, *Three-Dimensional Collective Charge Excitations in Electron-Doped Copper Oxide Superconductors*, Nature (London) **563**, 374 (2018).

[44] Matteo Rossi, Riccardo Arpaia, Roberto Fumagalli, Marco Moretti Sala, Davide Betto, Kurt Kummer, Gabriella M. De Luca, Jeroen van den Brink, Marco Salluzzo, Nicholas B. Brookes, Lucio Braicovich, and Giacomo Ghiringhelli, *Experimental Determination of Momentum-Resolved Electron-Phonon Coupling*, Phys. Rev. Lett. **123**, 027001 (2019).

[45] Lucio Braicovich, Matteo Rossi, Roberto Fumagalli, Yingying Peng, Yan Wang, Riccardo Arpaia, Davide Betto, Gabriella M. De Luca, Daniele Di Castro, Kurt Kummer, Marco Moretti Sala, Mattia Pagetti, Giuseppe Balestrino, Nicholas B. Brookes, Marco Salluzzo, Steven Johnston, Jeroen van den Brink, and Giacomo Ghiringhelli, *Determining the Electron-Phonon Coupling in Superconducting Cuprates by Resonant Inelastic X-Ray Scattering: Methods and Results on* $Nd_{1+x}Ba_{2-x}Cu_3O_{7-\delta}$, Phys. Rev. Research **2**, 023231 (2020).

[46] M. Moretti Sala, Valentina Bisogni, C. Aruta, G. Balestrino, H. Berger, N. B. Brookes, G. M. De Luca, D. Di Castro,

M. Grioni, M. Guarise *et al.*, *Energy and Symmetry of dd Excitations in Undoped Layered Cuprates Measured by Cu L_3 Resonant Inelastic X-Ray Scattering*, New J. Phys. **13**, 043026 (2011).

[47] Luuk J. P. Ament, Michel van Veenendaal, Thomas P. Devereaux, John P. Hill, and Jeroen van den Brink, *Resonant Inelastic X-Ray Scattering Studies of Elementary Excitations*, Rev. Mod. Phys. **83**, 705 (2011).

[48] O. K. Andersen, S. Y. Savrasov, O. Jepsen, and A. I. Liechtenstein, *Out-of-Plane Instability and Electron-Phonon Contribution to s- and d-Wave Pairing in High-Temperature Superconductors; LDA Linear-Response Calculation for Doped* $CaCuO_2$ *and a Generic Tight-Binding Model*, J. Low Temp. Phys. **105**, 285 (1996).

[49] K. W. Plumb, A. T. Savici, G. E. Granroth, F. C. Chou, and Young-June Kim, *High-Energy Continuum of Magnetic Excitations in the Two-Dimensional Quantum Antiferromagnet* $Sr_2CuO_2Cl_2$, Phys. Rev. B **89**, 180410(R) (2014).

[50] Y. Y. Peng, E. W. Huang, R. Fumagalli, M. Minola, Y. Wang, X. Sun, Y. Ding, K. Kummer, X. J. Zhou, N. B. Brookes, B. Moritz, L. Braicovich, T. P. Devereaux, and G. Ghiringhelli, *Dispersion, Damping, and Intensity of Spin Excitations in the Monolayer* $(Bi,Pb)_2(Sr,La)_2CuO_{6+\delta}$ *Cuprate Superconductor Family*, Phys. Rev. B **98**, 144507 (2018).

[51] Mathieu Le Tacon, G. Ghiringhelli, J. Chaloupka, M. Moretti Sala, V. Hinkov, M. W. Haverkort, Matteo Minola, M. Bakr, K. J. Zhou, S. Blanco-Canosa *et al.*, *Intense Paramagnon Excitations in a Large Family of High-Temperature Superconductors*, Nat. Phys. **7**, 725 (2011).

[52] M. Minola, G. Dellea, H. Gretarsson, Y. Y. Peng, Y. Lu, J. Porras, T. Loew, F. Yakhou, N. B. Brookes, Y. B. Huang, J. Pelliciari, T. Schmitt, G. Ghiringhelli, B. Keimer, L. Braicovich, and M. Le Tacon, *Collective Nature of Spin Excitations in Superconducting Cuprates Probed by Resonant Inelastic X-Ray Scattering*, Phys. Rev. Lett. **114**, 217003 (2015).

[53] Valentina Bisogni, Stefanos Kourtis, Claude Monney, Kejin Zhou, Roberto Kraus, Chinnathambi Sekar, Vladimir Strocov, Bernd Büchner, Jeroen van den Brink, Lucio Braicovich, Thorsten Schmitt, Maria Daghofer, and Jochen Geck, *Femtosecond Dynamics of Momentum-Dependent Magnetic Excitations from Resonant Inelastic X-Ray Scattering in* $CaCu_2O_3$, Phys. Rev. Lett. **112**, 147401 (2014).

[54] Hidemaro Suwa, Arnab Sen, and Anders W. Sandvik, *Level Spectroscopy in a Two-Dimensional Quantum Magnet: Linearly Dispersing Spinons at the Deconfined Quantum Critical Point*, Phys. Rev. B **94**, 144416 (2016).

[55] F. D. M. Haldane, *Fractional Statistics in Arbitrary Dimensions: A Generalization of the Pauli Principle*, Phys. Rev. Lett. **67**, 937 (1991).

[56] J. Schlappa, K. Wohlfeld, K. J. Zhou, M. Mourigal, M. W. Haverkort, V. N. Strocov, L. Hozoi, C. Monney, S. Nishimoto, S. Singh *et al.*, *Spin-Orbital Separation in the Quasi-One-Dimensional Mott Insulator* Sr_2CuO_3, Nature (London) **485**, 82 (2012).

[57] L. Braicovich, J. van den Brink, V. Bisogni, M. Moretti Sala, L. J. P. Ament, N. B. Brookes, G. M. De Luca, M. Salluzzo, T. Schmitt, V. N. Strocov, and G. Ghiringhelli, *Magnetic Excitations and Phase Separation in the Underdoped* $La_{2-x}Sr_xCuO_4$ *Superconductor Measured by Resonant Inelastic X-Ray Scattering*, Phys. Rev. Lett. **104**, 077002 (2010).

[58] M. W. Haverkort, *Theory of Resonant Inelastic X-Ray Scattering by Collective Magnetic Excitations*, Phys. Rev. Lett. **105**, 167404 (2010).

[59] Chunjing Jia, Krzysztof Wohlfeld, Yao Wang, Brian Moritz, and Thomas P. Devereaux, *Using RIXS to Uncover Elementary Charge and Spin Excitations*, Phys. Rev. X **6**, 021020 (2016).

[60] Umesh Kumar, Abhishek Nag, Jiemin Li, H. C. Robarts, A. C. Walters, Mirian García-Fernández, R. Saint-Martin, A. Revcolevschi, Justine Schlappa, Thorsten Schmitt *et al.*, *Unraveling Higher-Order Corrections in the Spin Dynamics of RIXS Spectra*, arXiv:2110.03186.

[61] J.-Y. P. Delannoy, M. J. P. Gingras, P. C. W. Holdsworth, and A.-M. S. Tremblay, *Low-Energy Theory of the* $t-t'-t''-U$ *Hubbard Model at Half-Filling: Interaction Strengths in Cuprate Superconductors and an Effective Spin-Only Description of* La_2CuO_4, Phys. Rev. B **79**, 235130 (2009).

[62] N. M. R. Peres and M. A. N. Arajo, *Spin Waves in* La_2CuO_4*: Band Structure and Correlation Effects*, Phys. Status Solidi (b) **236**, 523 (2003).

[63] C. B. Larsen, A. T. Rømer, S. Janas, F. Treue, B. Mønsted, N. E. Shaik, H. M. Rønnow, and K. Lefmann, *Exact Diagonalization Study of the Hubbard-Parametrized Four-Spin Ring Exchange Model on a Square Lattice*, Phys. Rev. B **99**, 054432 (2019).

[64] S. Skanthakumar, H. Zhang, T. W. Clinton, W. H. Li, J. W. Lynn, Z. Fisk, and S.-W. Cheong, *Magnetic Phase Transitions and Structural Distortion in* Nd_2CuO_4, Physica (Amsterdam) **160C**, 124 (1989).

[65] S. Toth and B. Lake, *Linear Spin Wave Theory for Single-Q Incommensurate Magnetic Structures*, J. Phys. Condens. Matter **27**, 166002 (2015).

[66] S. M. Hayden, G. Aeppli, T. G. Perring, H. A. Mook, and F. Doğan, *High-Frequency Spin Waves in* $YBa_2Cu_3O_{6.15}$, Phys. Rev. B **54**, R6905 (1996).

[67] J. M. Tranquada, G. Shirane, B. Keimer, S. Shamoto, and M. Sato, *Neutron Scattering Study of Magnetic Excitations in* $YBa_2Cu_3O_{6+x}$, Phys. Rev. B **40**, 4503 (1989).